Heliyon 9 (2023) e17700

Contents lists available at ScienceDirect

Heliyon

journal homepage: www.cell.com/heliyon

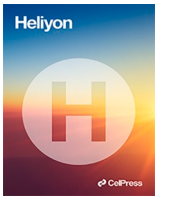

Beet leaf (beta vulgaris L.) extract attenuates iron-induced testicular toxicity: Experimental and computational approach

Oluwafemi Adeleke Ojo [a,*], Anthonia Oluyemi Agboola [b], Olalekan Bukunmi Ogunro [c], Matthew Iyobhebhe [d], Tobiloba Christiana Elebiyo [d], Damilare Emmanuel Rotimi [d], Joy Folashade Ayeni [d], Adebola Busola Ojo [e], Adeshina Isaiah Odugbemi [a,f,g], Samuel Ayodele Egieyeh [g,h], Olarewaju Michael Oluba [d]

[a] *Phytomedicine, Molecular Toxicology, and Computational Biochemistry Research Laboratory (PMTCB-RL), Department of Biochemistry, Bowen University, Iwo, 232101, Nigeria*
[b] *Department of Biochemistry, Wesley University, Ondo, Nigeria*
[c] *Department of Biological Sciences, KolaDaisi University, Ibadan, Nigeria*
[d] *Department of Biochemistry, Landmark University, Omu-Aran, Nigeria*
[e] *Department of Biochemistry, Ekiti State University, Ado-Ekiti, Nigeria*
[f] *South African National Bioinformatics Institute, Faculty of Natural Sciences, University of the Western Cape, Cape Town, South Africa*
[g] *National Institute for Theoretical and Computational Sciences (NITheCS), Cape Town, South Africa*
[h] *School of Pharmacy, University of Western Cape, Cape Town, South Africa*

A R T I C L E I N F O

Keywords:
Beta vulgaris leaf
Redox imbalance
Testicular toxicity
Computational models

A B S T R A C T

The purpose of this study was to investigate the protective effect of Beta vulgaris leaf extract (BVLE) on Fe2+-induced oxidative testicular damage via experimental and computational models. Oxidative testicular damage was induced via incubation of testicular tissue supernatant with 0.1 mM FeSO4 for 30 min at 37 °C. Treatment was achieved by incubating the testicular tissues with BVLE under the same conditions. The catalase (CAT), superoxide dismutase (SOD), glutathione (GSH), malondialdehyde (MDA), and nitric oxide (NO) levels, acetylcholinesterase (AChE), sodium-potassium adenosine triphosphatase (Na+/K + ATPase), ecto-nucleoside triphosphate diphosphohydrolase (ENTPDase), glucose-6-phosphatase (G6Pase), and fructose-1,6-bisphosphatase (F-1,6-BPase) were all measured in the tissues. We identified the bioactive compounds present using high-performance liquid chromatography (HPLC). Molecular docking and dynamic simulations were done on all identified compounds using a computational approach. The induction of testicular damage ($p < 0.05$) decreased the activities of GSH, SOD, CAT, and ENTPDase. In contrast, induction of testicular damage also resulted in a significant increase in MDA and NO levels and an increase in ATPase, G6Pase, and F-1,6-BPase activities. BVLE treatment ($p < 0.05$) reduced these levels and activities compared to control levels. An HPLC investigation revealed fifteen compounds in BVLE, with quercetin being the most abundant. The molecular docking and MDS analysis of the present study suggest that schaftoside may be an effective allosteric inhibitor of fructose 1,6-bisphosphatase based on the interacting residues and the subsequent effect on the dynamic loop conformation. These findings indicate that B. vulgaris

* Corresponding author. Department of Biochemistry, Bowen University, Iwo, 232101, Nigeria.
E-mail address: oluwafemiadeleke08@gmail.com (O.A. Ojo).

https://doi.org/10.1016/j.heliyon.2023.e17700
Received 21 September 2022; Received in revised form 7 June 2023; Accepted 26 June 2023
Available online 30 June 2023

can protect against Fe2+-induced testicular injury by suppressing oxidative stress, acetylcholinesterase, and purinergic activities while regulating carbohydrate dysmetabolism.

1. Introduction

Testicular dysfunction is projected to increase from 152 million cases in 1995 to about 322 million cases by 2025 [1]. Testicular dysfunction is the inability to obtain or maintain an erection for sufficient sexual performance. This has devastating effects on men as it hampers their sexual satisfaction and experiences [2–4]. Testicular dysfunction could be triggered by environmental pollutant, especially heavy metals such as; lead (Pb) and iron (Fe) [5–7]. These metals work majorly by disrupting redox balance which consequently disrupts steroidogenesis and spermatogenesis in humans and animals [5].

Oxidative stress has been implicated in about 50% of cases of testicular dysfunction [7]. This is because the testes and their sperm cells majorly contains unsaturated fatty acids that expose them to attack by free radicals [8]. Oxidative stress in the testes could: reduce sperm count and motility and damage sperm motility [9]; induce tissue damage in the spermatozoa [10]; and cause fragmentation in sperm DNA [11]. Oxidative stress in the testes also causes dysfunctions in some cholinergic, purinergic, and glucose metabolizing proteins, affecting neurotransmission, energy metabolism, and blood supply [7,12].

The pathophysiology and development of oxidative testicular dysfunction have been linked to alterations in testicular glucose metabolism that result in decreased glycolytic activity [6]. Anaerobic glycolysis is the main metabolic pathway for spermatic cells' energy metabolism, however it is typically disrupted in severe metabolic illnesses such diabetes, testicular cancer, and obesity [7].

Medicinal plants and their natural products are utilized globally for the treatment of numerous diseases, including testicular dysfunction. Beta vulgaris, commonly known as beet, is from the subspecies vulgaris of the Amaranthaceae family. The plant is considered to be relatively safe with an estimated acute lethal dose (LD50) higher than 2000 mg/kg in rodents [13,14]. The roots of the beet plant have been shown to possess hepatoprotective, nephroprotective, anti-inflammatory, anti-diabetic, and antimicrobial properties [15–18]. The beet leaf, which is often discarded, has also been reported to be relatively safe (LD50 $>$ 2000 mg/kg) and to possess hypoglycemic, immunomodulatory, and antioxidant effects [13]. However, there is a paucity of data on the effect of the beet leaf on iron-induced testicular toxicity. Therefore, this study investigated the therapeutic potential of B. vulgaris leaf against iron-induced testicular toxicity by exploring its effect on redox imbalance, cholinergic, purinergic, and glucose metabolizing enzyme activities. Furthermore, bioactive compounds identified from B. vulgaris leaf were subjected to molecular docking and molecular simulation studies.

2. Materials and methods

2.1. Beet leaf collection

In December 2021, the beet plant's leaves were purchased from a Jos Terminal market, Plateau State, Nigeria. The plant was verified at Forestry Research Institute of Nigeria in Ibadan with herbarium number FHI 114105.

2.2. Beet leaf extraction

The plants were thoroughly cleaned, cut into small pieces, and allowed to dry before being ground with an industrial miller into powder. 500 mL of water were steeped for 48 h with 50 g of beet powder. Muslin cloth was used to sieve the solution, and was concentrated in a steam bath at 45 °C. The yield of 34.83 g was obtained.

2.3. Antioxidant studies

2.3.1. Evaluation of nitric oxide (NO) scavenging activity of BVLE

The NO scavenging ability of B. vulgaris leaf extract (BVLE) was assessed using the procedure illustrated by Alam et al. [19] with slight modifications. In brief, 1 mL of 10 mM sodium nitroprusside in phosphate buffered saline (pH 7.4) was mixed with 250 μL of plant samples at varying concentrations. The mixture was left to stand at room temperature for 150 min and an equal volume of Griess reagent was added to the mixture. The setup was incubated again at room temperature for 30 min, and the nitric oxide capacity of the extract was measured at 546 nm spectrophotometrically. The percentage inhibition was calculated as follows:

$$Percentage\ inhibitation\ (\%) = \left[\frac{Abs\ of\ sample}{Abs\ of\ control}\right]$$

2.3.2. Evaluation of free radical scavenging activity of BVLE

DPPH assay of BVLE was assessed following the procedure illustrated by Ref. [20]. In this experiment, 0.5 mL of varying concentrations of the aqueous leaf extract were mixed with 1 mL of freshly prepared 0.2 mM DPPH solution in absolute methanol. After 30 min of incubation at 25 °C, the absorbance at 517 nm was measured. The following formula was used to get the percentage inhibition: $Percentage\ inhibitation\ (\%) = 1 - \left[\frac{Abs\ of\ sample}{Abs\ of\ control}\right]$.

2.3.3. Evaluation of ferric-reducing antioxidant power of BVLE

FRAP assay of BVLE was determined by the procedure illustrated by Mzoughi et al. [20] with slight modifications. In brief, 250 μL of varying concentrations of the plant sample were added to 0.625 mL of 0.2 M phosphate buffer (pH 6.6) and 0.625 μL of 1% K3Fe(CN) 6. Following incubation at 500 °C for 20 min and subsequent cooling of the reaction mixture at room temperature, 0.625 mL of 10% trichloroacetic acid was added to halt the reaction. Afterwards, the mixture was centrifuged at 2000g for 10 min; 0.625 mL of the supernatant was pipetted into a clean test tube containing 0.625 mL of distilled water and 125 μL of 1% FeCl3. The mixture was let to stay for 10 min and the absorbance was read at 700 nm against a blank.

2.3.4. Evaluation of iron (Fe) chelating activity of BVLE

Iron (Fe) chelating assay of BVLE was determined using the methods described by Alam, Bristi and Rafiquzzaman [19] with slight modifications. Approximately 500 μL of 0.2 mM FeCl3 was added to 100 μL varying concentrations of the beet extract and standard (EDTA). The reaction was activated by adding 200 μL of 5 mM ferrozine to the mixture, which was subsequently incubated at 25 °C for 10 min. The absorbance was read at 562 nm.

2.3.5. Hydroxyl (OH) radical scavenging activity of BVLE

This study was carried out using the method described by Ref. [7]. A reaction mixture was prepared by sequentially reacting 100 μL of the beet extract with 150 μL of 20 mM deoxyribose, 250 μL of phosphate buffered saline, 100 μL of 500 μM FeSO4 and 100 μL of 1% H2O2. The mixtures were incubated for 30 min at 370C, after which 200 μL of 10% TCA and 600 μL of 0.25% TBA were added. Afterwards, the mixture was boiled for 20 min and then left to cool at room temperature. Ascorbic acid was used as the control solution. The absorbance was read at 532 nm, and the radical scavenging activity was calculated using the formula:

$$\%\ radical\ scavenging = \left[\frac{Abs\ of\ control - (Abs\ of\ sample\ with\ deoxyribose - Abs\ of\ sample\ without\ deoxyrise}{Abs\ of\ control}\right]$$

2.3.6. Evaluation of the total antioxidant capacity (TAC) of BVLE

TAC assay of BVLE was assessed following the procedure described by Rahman et al. [21]. 250 μL of varying concentrations of beet samples and standards were mixed into the test tubes with 1.5 mL of a reaction mixture containing 0.6 M H2SO4, 0.028 M sodium phosphate, and 1% ammonium molybdate. The test tubes were then incubated at 95 °C for 10 min to complete the reaction. After cooling at room temperature, absorbance was read at 695 nm against a blank solution containing 250 μL of the solvent used for the samples and 1.5 mL of the reaction mixture.

2.3.7. Ex-vivo experiments

2.3.7.1. Animals and organ harvesting. We bought male rats (200–250 g) from the Department of Biochemistry, University of Ilorin. After being fasted overnight the rats were anesthetized with halothane and the testes were harvested. The harvested testes were homogenized and centrifuged at 15,000 rpm and 40 °C. The supernatant was separated into tubes for ex-vivo investigations. The study received approval from the LMU Animal Ethics Committee (LUAC/BCH/2022/0002 A). The study was also reported in accordance with ARRIVE standards.

2.3.7.2. Testicular damage induction. The techniques described by Refs. [7,22] were employed to generate testicular damage ex vivo with slight modifications. In a nutshell, 100 μL of 0.1 mM FeSO4 was added to 200 μL of the testes supernatant that contained varied concentrations (15–240 μg/mL) of BVLE or gallic acid. The solutions were used for biochemical examinations following a 30-mins incubation period at 37 °C. The negative control contains only the testes supernatant and FeSO4, while the normal control contains only the testes supernatant.

2.3.7.3. Antioxidant activities measurement

2.3.7.3.1. Catalase (CAT) activity of BVLE. With minor adjustments, CAT activity of BVLE was assessed in accordance with the description in Ref. [22]. Twenty (20)mL of testes supernatant containing varying concentrations of BVLE were mixed with 780 mL of 50 mM phosphate buffer. The absorbance was then read at 240 min for 3 min at a 1 min interval after adding 300 μL of 2 M H2O2.

2.3.7.3.2. Reduced glutathione level. As depicted by Salau et al. [23], 600 mL of 10% trichloroacetic acid was added to the testes lysates to deproteinize them. For 10 min, the solution was centrifuged at 3500 rpm 100 mL of Ellman reagent was added to the solution after 500 mL of the sample was transferred into a test tube. After 5 min of incubation at 25 °C, the absorbance was read at 415 nm.

2.3.7.3.3. Superoxide dismutase (SOD) activity. The technique of [24] was used to ascertain the activity of SOD. 50 μL of the testes lysates containing various quantities of BVLE were combined with 50 mL of freshly prepared 1.6 mM 6-hydroxydopamine (6-HD) and 350 mL of 0.1 mM diethylenetriaminepentaatic acid. At a 1-min interval, absorbance was read at 492 nm for 5 min.

2.3.7.3.4. Level of lipid peroxidation. The ability of BVLE to reduce lipid peroxidation was also evaluated using the technique outlined by Ref. [22]. 100 L of the testes lysates containing various concentrations of BVLE were added sequentially to 375 μL of 20% acetic acid, 1000 μL of 0.25% thiobarbituric acid, and 100 μL of 8.1% SDS. In a water bath, the reaction solution was boiled for 60 min at 95 °C. The absorbance was measured at 532 nm after allowing the reaction solution to cool to 25 °C.

2.4. Purinergic and cholinergic actions

The methods outlined by Refs. [6,7,25] were used to measure the acetylcholinesterase, ecto-nucleoside triphosphate diphosphohdrolase (ENTPDase) and ATPase, activities.

2.4.1. Acetylcholinesterase activity

100 μL of testes supernatant mixed with varying concentrations of BVLE were added to 50 μL of Ellman's reagent (3.3 mM, pH 7.0) and 250 μL of 100 mM sodium phosphate buffer based on the protocol defined by Ref. [7]. 50 μL of 50 mM acetylcholine iodide was added to the reaction solution after it had been incubated at 25 °C for 20 min. The absorbance was read quickly at 412 nm at 3 min intervals for 15 min.

2.4.2. Na/K + ATPase enzyme activity

A small modification of the technique described by 25] was used to determine Na/K + ATPase activity. To 200 μL of the testes lysate containing various concentrations of BVLE were combined with 1.3 μL of 0.1 M Tris-HCl buffer, 200 μL of 5 mM KCl, and 40 μL of 50 mM ATP. Using a mechanical shaker, the reaction solution was incubated at 37 °C for 30 min before 1 mL of distilled H2O and 1 mL of 1.25% ammonium molybdate were added. After that, 1 mL of 9% ascorbic acid was added to the solution, and it was left untouched for 30 min. At 660 nm, the absorbance was then measured.

2.4.3. E-NTPDase enzyme activity

Based on the protocol defined by Ref. [7], 40 μL of testes lysates containing differing concentrations of BVLE were added to 400 μL of a reaction combination solution (containing: 10 mM glucose, 0.1 mM EDTA, 1.5 mM CaCl2, 5 mM KCl, and 1.5 mM CaCl2. 225 mM sucrose and 45 mM Tris-HCl). T After that, the solutions were incubated for 10 min at 37 °C. Afterwards, 40 μL of 50 mM ATP was added and the blend was additionally incubated at 37 °C in a mechanical shaker. 400 L of 10% TCA was added to the solution to stop the reaction. After 10 min of incubation on ice, the solution was read for absorbance at 600 nm.

2.5. Glucose metabolizing enzyme activities

2.5.1. Glucose-6-phosphatase

The procedure outlined by Ref. [26] was used to measure glucose-6-phosphatase activity. 100 μL of the testes lysates were combined with 300 μL of 0.5 M maleic acid buffer (pH 6.5), 100 μL of 0.1 M glucose-6-phosphate, and 100 μL of BVLE in different concentration. After cooling in an ice bath, the solution was left to incubate at 37 °C for 15 min. The addition of 1 mL of 10% TCA halted the reaction while it was still on ice. After 10 min of centrifuging at 3000 rpm, the supernatant's absorbance was measured at 340 nm.

2.5.2. Fructose-1,6-bis phosphatase activity

Fructose-1,6-bis phosphatase activity was determined by modifying the approaches outlined by Refs. [7,26]. A total of 1.2 mL of 0.1 M Tris-HCL buffer (pH 7.0), 100 μL of 0.05 M fructose, 250 μL of 0.1 M KCl, 250 μL of 0.1 M EDTA, and 100 μL of 0.1 M MgCl2 were combined with the testes supernatants containing varying concentrations of BVLE. For 15 min, the mixture was left to incubate at 37 °C. After that, 100 μL of 10% TCA was used to stop the reaction. The solution was then centrifuged for 10 min at 3000 rpm. The absorbance was measured at 680 nm after 1 mL of the supernatant was reacted with 1 mL of 9% ascorbic acid and kept warm at 37 °C for 30 min.

2.5.3. In silico studies

In this study, ligand preparation, molecular docking, and Prime-MMGBSA calculations were performed on the 15 compounds identified, using the fructose 1,6-bisphosphatase (F-1,6-BP) crystal structure retrieved from the Protein Data Bank as a target. Based on the free energy of binding to the target, the top two compounds were selected for molecular dynamics simulations (MDS) to investigate the details of their interactions.

2.5.4. Ligand preparation

Energy minimization of compounds was conducted using the OPLS4 (Optimized Potentials for Liquid Simulations) force field using the LigPrep Module in Maestro version 13.0 of the Schrodinger Suite 2021–4 release (LigPrep, Schrödinger, LLC, New York, NY, 2021). Using the Epik ionization tool [27], the ionization state was established at a pH range of 7.4 ± 2.0. All the 3D conformers generated for each ligand were used for the docking procedure.

2.6. Target selection and preparation

The crystal structure of human FBP in complex with fructose 1,6-phosphate and an indole allosteric inhibitor was retrieved from the protein data bank (PDB) 7EZF [28]. The Protein Preparation Wizard [29] in the Maestro v13.0 was utilized to prepare the protein. The protein was preprocessed by assigning bond orders and adding hydrogen. Protonation and metal charge state were generated for ligands using Epik as well at pH 7.4 ± 2.0. Chain D of the homotetramer FBP was selected for refinement due to its high ranking for goodness of fit for its bound native ligand. The protein was then refined by predicting the pKa values of ionizable groups using PropKa at a pH of 7.4 and the crystallographic water molecules were removed. Restrained minimization was performed using the OPLS4 force

field.

2.7. Receptor grid generation

The Glide Receptor Grid Generation module was used to create a grid box around the centroid of the co-crystallized ligand bound at the allosteric site on the prepared protein. The grid center coordinates on the receptor were set at x = 5.94, y = -8.40, and z = 54.62, and the inner box defines the diameter midpoint restrain of each ligand to be docked, set at 11 Å × 11 Å x 11 Å.

2.8. Molecular docking

To predict the binding pose of ligands, an extra precision (XP) Glide docking approach was used to dock the prepared and minimized ligands into the generated receptor grid on the prepared FBP. Epik state penalties were factored into the docking score computation. The docking computations used the OPLS4 force field and the ligand interaction diagram module of the Schrodinger suite to examine the complexes' 2D interactions.

2.9. Post-docking MMGBSA calculations

The Prime-MMGBSA panel of the Prime module in the Schrodinger Suite 2020–4 release was used to calculate ligand binding free energies using molecular mechanics with generalized Born and surface area solvation (MM-GBSA) technology. The pose viewer file from the molecular docking output serves as the input structure for the Prime-MMGBSA calculation. The Variable-dielectric generalized Born model (VSGB) was selected as the solvation model, which incorporates residue-dependent effects.

The binding free energy ΔGbind is estimated as

$$\Delta Gbind = \Delta EMM + \Delta Gsolv + \Delta GSA$$

Where ΔEMM is the difference in energy between the complex structure and the sum of the energies of the separated ligand and protein, ΔGsolv is the difference in the GBSA solvation (implicit/continuum solvation model) energy of the complex and the sum of the solvation energies for the separated ligand and protein, and ΔGSA is the difference in the surface area energy for the complex and the sum of the surface area energies for the separated ligand and protein [30]. The top two ligands with the best binding free energies to the protein were considered for MDS.

2.10. Molecular dynamics simulations

The molecular dynamics simulations were performed with the Desmond package in the Schrodinger Suite 2021–4 release. The system was first set up with the System Builder module in the Desmond package. The selected docked complexes were each placed in an orthorhombic box with a buffered distance of 10 Å beyond the complexes. The complexes were solvated with a four-site water model, TIP4P. The system was neutralised by adding sodium and chloride counter ions and was then set at 0.15 M NaCl to mimic the physiological state. The system was equilibrated with NPT ensemble class at a temperature of 300 K and a pressure of 1.01325 bar using a Nose-Hoover chain thermostat and a Martyna-Tobias-Klein barostat with isotropic coupling style. The MDS was performed for 200 ns, with trajectories recorded every 200 ps, for a total output of 1000 frames. The simulation's time step was set to 2.0 fs [31].

2.11. Post-MDS MMGBSA calculations

The free energy of ligand binding to protein was calculated for the trajectories using the Prime module in the Schrodinger suite via the python script, thermal_mmgbsa.py. The step size of 30 was used to generate the input structure files for the Prime module and the OPLS4 force field was applied. The binding energy of the receptor and ligand as calculated by the Prime Energy, a Molecular Mechanics + Implicit Solvent Energy Function (kcals/mol) [32].

$$\Delta Gbind = \Delta G(\text{Optimized Complex}) - \Delta G(\text{Optimized Free Ligand}) - \Delta G(\text{Optimized Free Receptor})$$

2.12. Data analysis

The data were analyzed with the help of the software Graphpad Prism version 9.0.1. To represent the descriptive data, the mean ± SD was utilized. Analysis of data was one using a one-way ANOVA utilizing Tukey's HSD post hoc test for comparison of means at $p < 0.05$.

3. Results

3.1. High performance liquid chromatography analysis of B. Vulgaris leaf

Chlorogenic acid, orientin, kaempferol, cryptochlorogenic acid, taxiphyllin, quercetin, apigenin, schaftoside, luteolin, catechin, iso-orientin, 6-glucosylapigenin, ferulic acid, *p*-coumaric acid, and benzoic acid were all identified in the chromatograms of the aqueous B. vulgaris leaf extract from the HPLC analysis (Table 1).

3.1.1. In vitro antioxidant activities

Fig. 1 represents the hydroxyl (OH), nitric oxide (NO), DPPH radical scavenging activities and ferric reducing antioxidant power (FRAP) of B. vulgaris leaf extract (BVLE). The BVLE displayed an increase in OH radical activity (Fig. 1a), which compared favorably with ascorbic acid. Likewise, BVLE revealed significant ($p < 0.05$) NO, DPPH, and FRAP (Fig. 1b, c, d). In addition, Fig. 2 shows the Fe2+ chelating ability and TAC of BVLE. The BVLE showed a dose-dependent increase in iron chelating ability (Fig. 2a) and total antioxidant activity (Fig. 2b), which compared well with EDTA and α-tocopherol, respectively.

3.1.2. Ex vivo antioxidant studies

Fig. 3a–d showed the reduced GSH level, SOD, and CAT activities with corresponding increased MDA in testicular tissues induced FeSO4. Treatment with BVLE dose-dependently ($p < 0.05$) reduced these activities in a significant manner.

3.2. Pro-inflammatory studies

Fig. 4 shows the increased NO level in testicular tissue incubation with FeSO4, suggesting a pro-inflammatory activity. NO level was markedly ($p < 0.05$) prevented on treatment with BVLE to near normal.

3.3. Cholinergic activities

Fig. 5 shows the effect of BVLE on testicular acetylcholinesterase (AChE) activity following induction of testicular tissues with FeSO4. AChE activity was markedly ($p < 0.05$) declined on treatment with BVLE.

3.4. Purinergic activity

As shown in Fig. 6a, the induction of testicular damage resulted in a significant ($p < 0.05$) increase in testicular ATPase activity and a corresponding decrease in *E*-NTPDase activity (Fig. 6b). The ATPase activity was markedly ($p < 0.05$) reduced on treatment with BVLE dose-dependently. Additionally, BVLE treatment increased testicular *E*-NTPDase activity significantly ($p < 0.05$) and dose-dependently (Fig. 6b).

3.5. Glucogenic activities

Fig. 7a and b shows a noteworthy ($p < 0.05$) increase of testicular G-6-Pase and F-1,6-BPase activities on the induction of oxidative damage by FeSO4. These glucogenic enzymes were markedly ($p < 0.05$) decreased in BVLE treatment groups.

Table 1
Compounds identified in aqueous Beta vulgaris leaf extract.

Bioactive compounds	Concentration (μg/1 g)
Chlorogenic acid	27.94
Cryptochlorogenic acid	59.28
Benzoic acid	18.51
p-Coumaric acid	8.54
Catechin	5.79
Iso-orientin	1.93
Orientin	2.24
Apigenin	1.79
6-Glycosylapigenin	2.39
Quercetin	191.12
Kaempferol	76.19
Luteolin	70.81
Schaftoside	2.70
Taxiphyllin	11.39
Ferulic acid	1.89

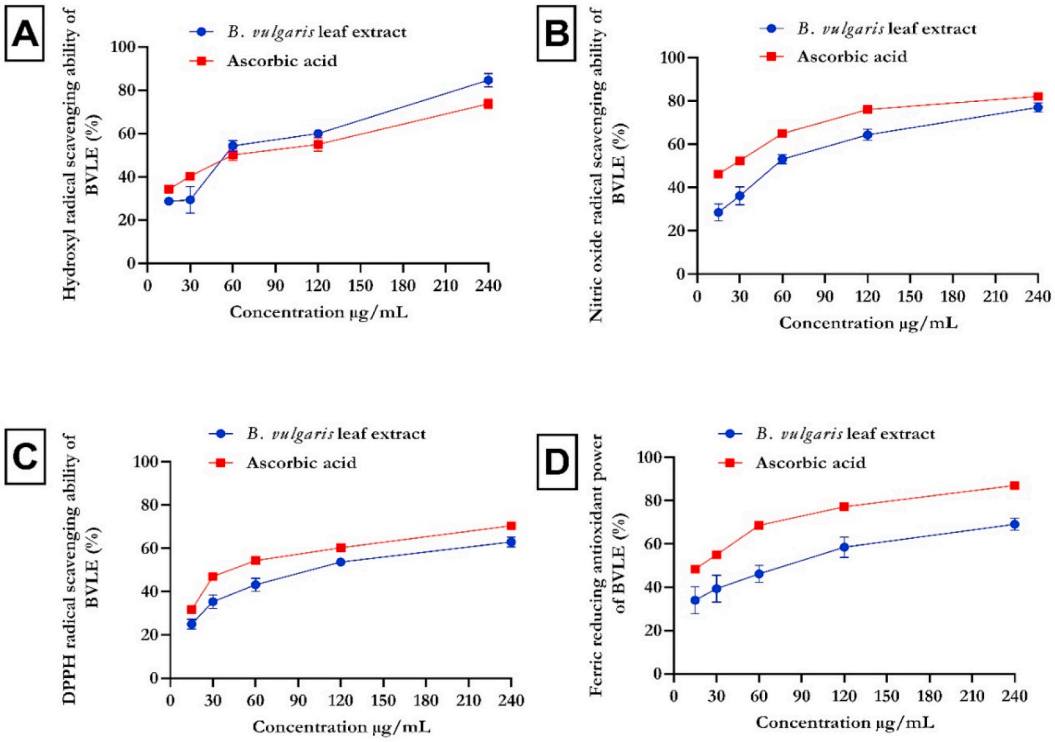

Fig. 1. In vitro antioxidant activity of aqueous extract of Beta vulgaris leaf on (A) Hydroxyl, (B) Nitric oxide, (C) DPPH, and (D) Ferric reducing power. Data expressed as mean ± SD (n = 3). Legends: BVLE: Beta vulgaris leaf extract.

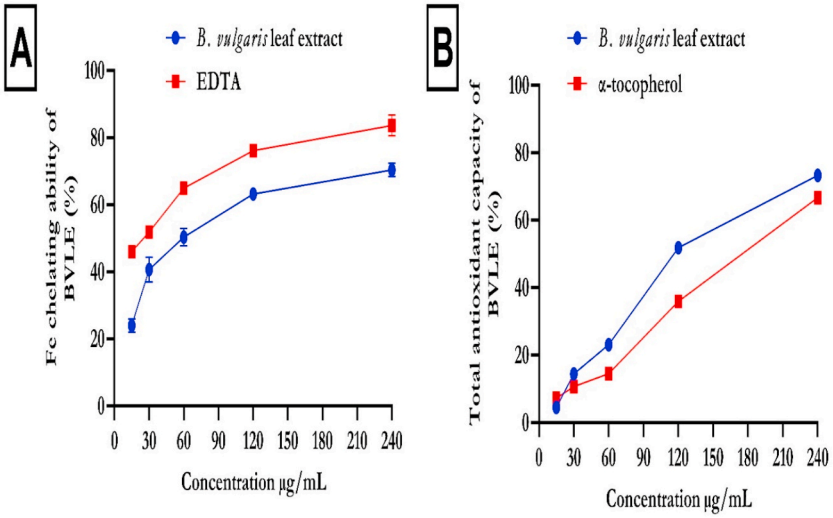

Fig. 2. Iron chelating ability and total antioxidant ability of B. vulgaris leaf extract. Data expressed as mean ± SD (n = 3). Legends: BVLE: Beta vulgaris leaf extract.

3.6. Computational studies

3.6.1. Post-docking binding free energy MM-GBSA

The top two molecules from our docking studies were schaftoside and quercetin (−53.82 and −51.18 kcal/mol, respectively) (Table 2). The two-dimensional interaction of the top two molecules with F-1,6-BP is shown in Fig. 8a, b.

A more detailed protein-ligand interaction was generated using Protein-Ligand Interaction Profiler and the presented in Tables 3 and 4.

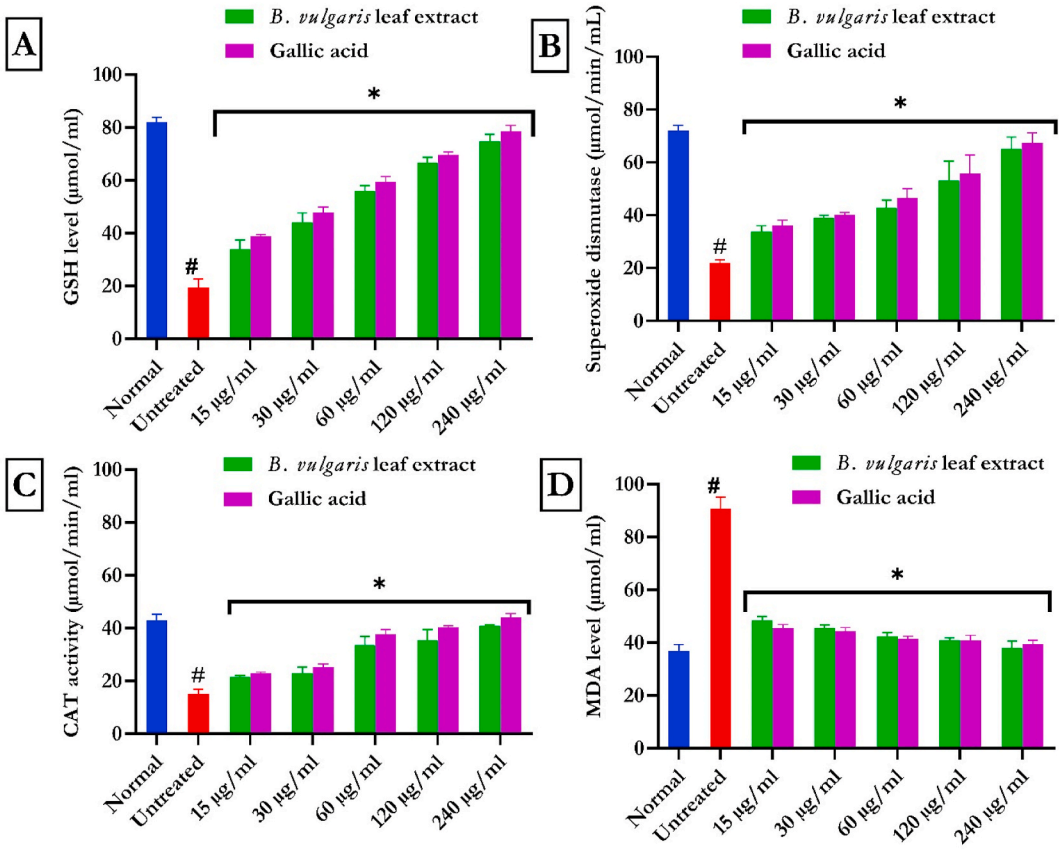

Fig. 3. Impact of B. vulgaris leaf on oxidative markers in Fe2+-induced testicular injury. Data were expressed as mean ± SD (n = 3). *Statistically significant compared to untreated testes; #statistically significant compared to the control cells ($p < 0.05$).

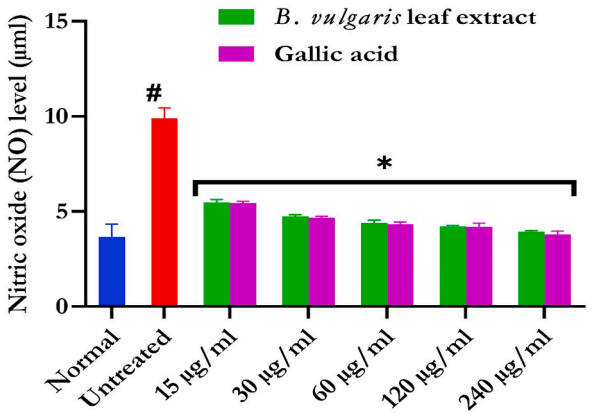

Fig. 4. Effect of B. vulgaris leaf on NO level in Fe2+-induced testicular injury. Data were expressed as mean ± SD (n = 3). *Statistically significant compared to untreated testes; #statistically significant compared to the control cells ($p < 0.05$).

3.6.2. Molecular dynamics simulation studies of hit compounds with F-1,6-BP

The higher RMSD was observed for FBP at about 130 ns (Fig. 9a) within the FBP-Schaftoside complex system. The Cα-FBP RMSD in the FBP-Quercetin complex system remained steady throughout the simulation period, indicating that quercetin does not appear to trigger structural changes in FBP (Fig. 9b). Furthermore, the proximity of quercetin to the bind pocket was poorer compared to schaftoside, as evidenced by the ligands' RMSD with respect to FBP (Fig. 9, blue lines).

Interestingly, comparing the FBP apoprotein RMSF data from a different MD simulation to the FBP RMSF data in the presence of Schaftoside revealed the site of the structural shift (Fig. 10). An examination of the simulation trajectory frame before and after the

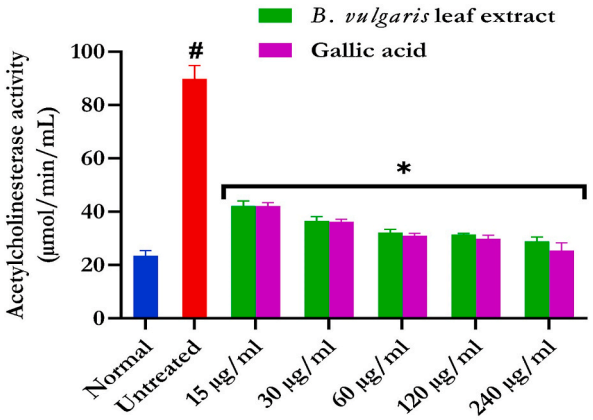

Fig. 5. Acetylcholinesterase activity of B. vulgaris leaf in Fe2+-induced testicular injury. Data were expressed as mean ± SD (n = 3). *Statistically significant compared to untreated testes; #statistically significant compared to the control cells ($p < 0.05$).

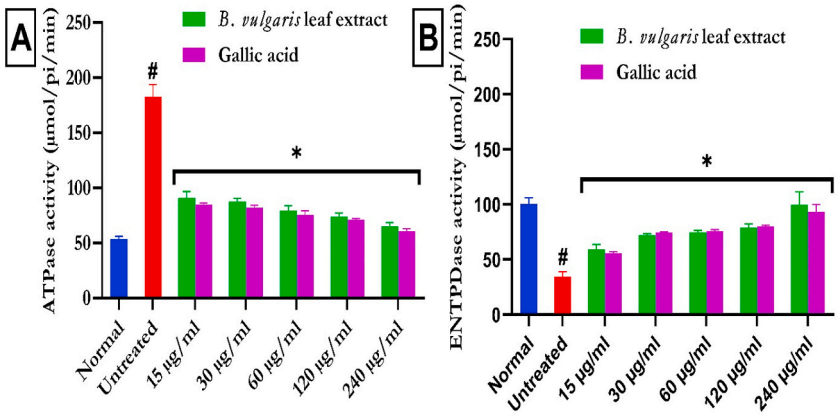

Fig. 6. ATPase and ENTPDase activities of B. vulgaris leaf in Fe2+-induced testicular injury. Statistical analysis was achieved via one-way ANOVA followed by Tukey's post hoc analysis. Data were expressed as mean ± SD (n = 3). The purinergic markers (ATPase and ENTPDase) in testis significantly (#$p < 0.05$) affected in FeSO4-induced control as compared to normal. However; the rest of the experimental treatment significantly (*$p < 0.05$) improved purinergic markers in FeSO4-induced testicular tissues. ATPase: adenylpyrophosphatase; ENTPDase: ecto-nucleoside triphosphate diphosphohydrolase.

RMSD increase further validates that it is indeed the dynamic loop that was distorted by about 12 Å (Fig. 11).

Hydrogen bonding interactions between FBP and schaftoside were shown to be dominant at THR_27, GLY_28, GLU_29, LEU_30 and THR_31 (Fig. 12a and b).

The hydrogen bonding interactions of schaftoside with the aforementioned residues were maintained for well over 70% of the duration of the entire simulation (across 4 points on the ligand, aiding stability) except for LEU_30 which was at 46% (Fig. 13a). Only one hydroxyl group on quercetin maintained a hydrogen bond interaction with two residues, GLY_28 and THR_31, implying a weaker interaction than schaftoside (Fig. 13b).

Furthermore, the result of the post-MDS MMGBSA calculations in Table 5 suggests schaftoside to have a significantly stronger free binding energy at −53.13 kcal/mol than quercetin at −31.09 kcal/mol ($P < 0.01$).

The ligands RMSD and radius of gyration suggests that the ligands' structures with respect to their heavy atoms were maintained throughout the simulation (Fig. 14).

4. Discussion

Infertility in men has long been a major concern, especially in families where having children is viewed as both a cultural necessity and a family value or obligation. Testicular dysfunction has been linked to a number of factors, with oxidative damage being one of the major pathologies [33]. Due to its accessibility and minimal side effects, folkloric medicine has long used medicinal plants to treat infertility. Recently, this practice has attracted a lot of attention. The present study looked into the ability of beet leaf extract to protect isolated testicular tissues from oxidative damage brought on by iron-II sulphate (FeSO4) via experimental and computational models.

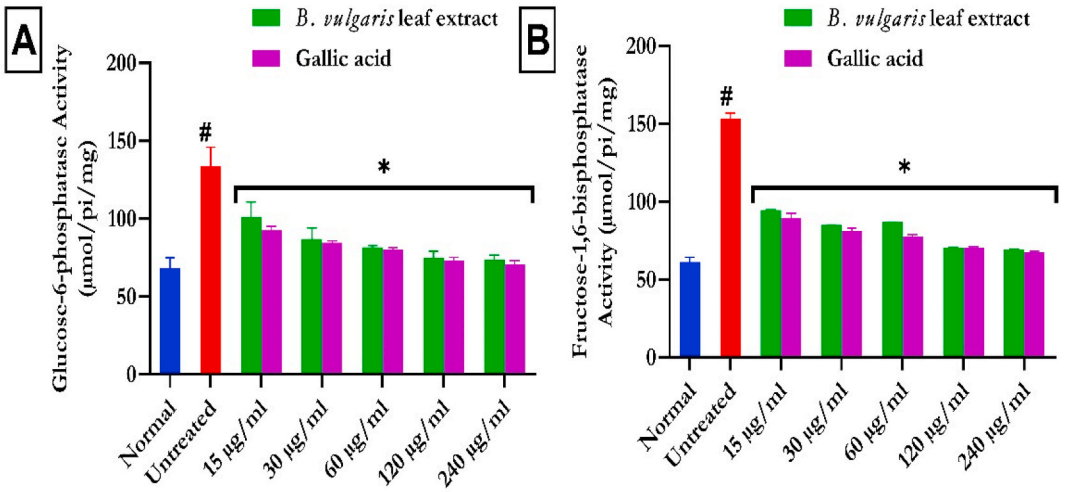

Fig. 7. Glucogenic activities of B. vulgaris leaf in Fe2+-induced testicular injury. Data were expressed as mean ± SD (n = 3). *Statistically significant compared to untreated testes; #statistically significant compared to the control cells ($p < 0.05$). G-6-Pase: glucose-6-phosphatase; F-1,6-BPase: fructose-1,6-bisphosphatase.

Table 2
Post-docking binding free energy MM-GBSA.

S/N	Compounds	ΔGbind (Kcal/mol)	ΔGbind Coulomb	ΔGbind Covalent	ΔGbind Hbond	ΔGbind Lipo	ΔGbind Solv_GB	ΔGbind vdW
1	Schaftoside	−53.82	−105.30	4.75	−3.94	−14.50	104.01	−38.84
2	Quercetin	−51.18	−108.83	3.09	−4.08	−7.09	99.99	−34.25
3	Luteolin	−50.16	−106.68	3.92	−4.00	−7.15	98.29	−34.54
4	Kaempferol	−48.98	−54.62	2.59	−2.82	−7.47	45.40	−32.07
5	Catechin	−46.06	−38.81	5.63	−3.78	−10.75	29.20	−27.06
6	Orientin	−44.71	−105.43	6.94	−4.21	−7.89	106.38	−40.50
7	Cryptochlorogenic acid	−44.33	1.30	3.08	−4.25	−14.08	0.33	−30.71
8	6-Glycosylapigenin	−44.14	−41.27	−0.32	−2.75	−10.51	39.04	−28.34
9	Chlorogenic acid	−42.13	−37.79	1.41	−3.70	−9.34	28.43	−21.14
10	Iso-orientin	−39.86	−36.48	0.57	−2.78	−10.21	38.72	−29.68
11	Apigenin	−36.23	−22.21	1.94	−2.45	−6.61	24.53	−31.41
12	Taxiphyllin	−35.69	−89.60	7.05	−3.43	−8.72	95.79	−36.78
13	Ferulic acid	−32.28	−14.98	1.54	−3.91	−11.36	26.00	−29.57
14	*p*-Coumaric acid	−25.85	−15.44	1.07	−3.70	−10.12	28.13	−25.78
15	Benzoic acid	−24.22	−17.11	0.42	−3.72	−6.04	19.88	−17.64

The phytoconstituents in fruits, herbs, and vegetables have been linked to their medicinal properties [34,35]. The beet leaf identified phytocompounds after HPLC analysis are well-known flavonoids and phenolics, and their potent antioxidant properties have been extensively researched [36–39]. The presence of these compounds may synergistically contribute to the reported antioxidant and other medicinal properties observed in this study.

The development of oxidative stress has been linked to increased free radical production [40]. Numerous studies have shown that medicinal plants can neutralize free radicals, preventing the onset of oxidative stress [41]. It's interesting to note that plants have antioxidant properties because of chemical compounds in their constituent parts that reduce the production of ROS, chelate pro-oxidant metallic ions, prevent the spread of free radicals, and speed up cellular repair processes [42]. This can be seen in the B. vulgaris leaf extracts' powerful ability to scavenge OH, NO, and DPPH radicals (Fig. 1a–c). This activity is consistent with earlier reports on B. vulgaris' capacity to mop up DPPH radical in vitro [38,43]. By chelating metal ions and reducing ferric iron, B. vulgaris demonstrated its antioxidant ability.

Research has shown that metals like arsenic [44] and iron [45] can cause testicular toxicity in males. In the Fenton reaction, Fe2+ interacts with H2O2 produced by mitochondrial respiratory pathways to produce hydroxyl and hydroperoxyl radicals. These chemical components could further set off chain reactions in the cell that would activate additional ROS [46]. Therefore, increased ROS levels compromise the antioxidant defense system's integrity, resulting in oxidative stress [47]. Following the induction of testicular oxidative injury, there was an occurrence of oxidative stress in the current study as demonstrated by the suppressed GSH level, catalase, and SOD activities, with concurrently high levels of MDA in the untreated tissues. These decreased levels and activities support a prior study that described the oxidative stress brought on by Fe2+ in testicular tissues [40]. This could be credited to the

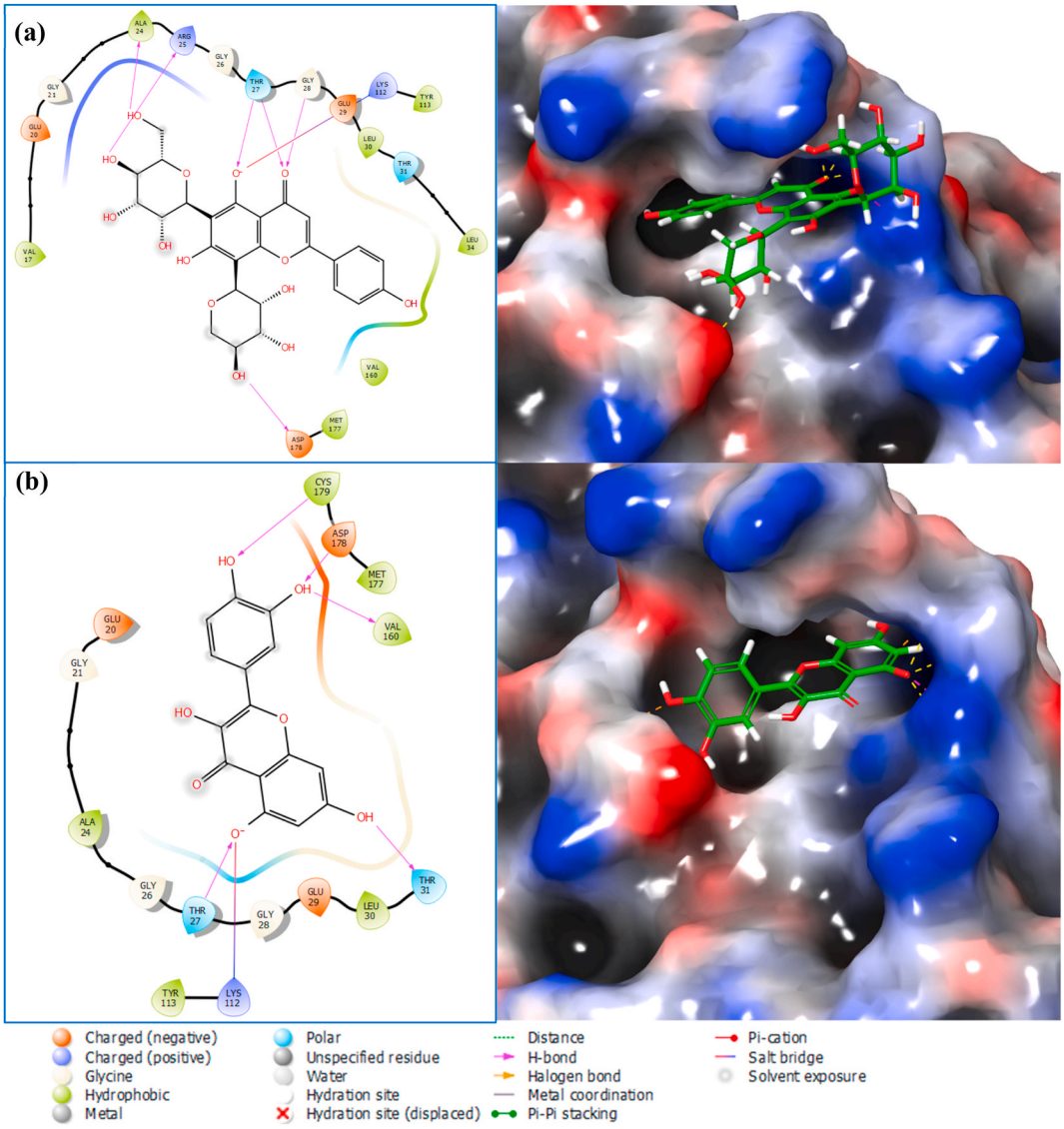

Fig. 8. 2-dimensional ligand interaction diagram of docked ligands (a) FBP-Schaftoside complex (b) FBP-Quercetin complex.

Table 3
Protein-ligand interaction of FBP-Schaftoside complex.

Hydrophobic Interactions				
Residue	AA	Distance		
20D	GLU	3.6		
30D	LEU	3.4		
Hydrogen Bonds				
Residue	Amino Acid	Distance H-A	Distance D-A	Donor Angle
24D	ALA	1.81	2.75	162.9
25D	ARG	1.75	2.72	169.55
27D	THR	1.9	2.78	143.49
27D	THR	1.86	2.79	163.11
28D	GLY	2.58	3.47	146.31
112D	LYS	3.01	3.46	108.21
178D	ASP	2.07	3.02	164.36

Table 4
Protein-ligand interaction of FBP-Quercetin complex.

Hydrophobic Interactions				
Residue	AA	Distance		
30D	LEU	3.84		
Hydrogen Bonds				
Residue	Amino Acid	Distance H-A	Distance D-A	Donor Angle
27D	THR	2.43	3.44	172.54
31D	THR	1.89	2.8	155.77
112D	LYS	2.91	3.54	121.24
160D	VAL	2.67	3.45	138.12
178D	ASP	2.22	3.21	167.69
179D	CYS	2.22	3.05	138.4

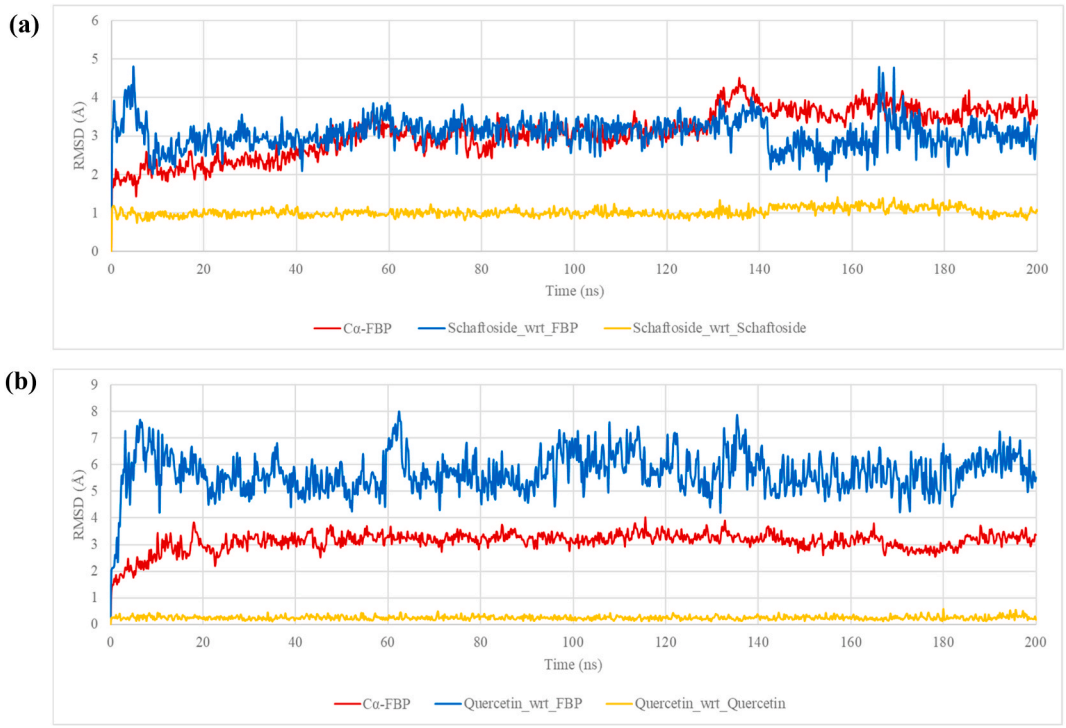

Fig. 9. RMSD from the MDS for 200ns with the first frame at time, t = 0 used as reference (a) FBP-Schaftoside complex system (b) FBP-Quercetin complex system.

Fenton's and Haber-Weiss reactions, which cause oxidative stress in iron-induced tissues [48].

The physiological level of NO is essential for male reproductive health [49]. NO controls the tunica albuginea's ability to contract and relax in the testes, providing the forces necessary to move sperm cells from the testes to the epididymis [50]. Although erection is ultimately caused by a slow increase in nitric oxide levels in penile tissues, testicles and other male tissues have been shown to suffer when the signaling molecule is present in significant amounts [51]. The progression of oxidative testicular toxicity has also been linked to pro-inflammation, with the production of ROS being acknowledged as a key factor [52]. As a result, the untreated tissue's increased NO level shows a pro-inflammatory effect. Therefore, it can be concluded that B. vulgaris extract has an anti-pro-inflammatory effect on oxidative testicular injury given the depleted NO level in the treated tissues.

The increased acetylcholinesterase activity in the Fe2+-induced testicular tissues shows that the induction of oxidative injury results in the breakdown of acetylcholine to acetate and choline. As a result, it shows a decreased acetylcholine level in the testicles, which denotes a change in testicular cholinergic activity since acetylcholine controls the activities of Leydig cells [53]. It has been suggested that oxidative stress contributes to an increase in acetylcholinesterase activity [54]. Testicular toxicity has been treated and managed using acetylcholinesterase activity inhibition [12,55]. Consequently, the decreased activity in BVLE-treated tissues points to enhanced testicular function, which is supported by the increased antioxidant activity observed in the testicular tissues. This supports studies that show acetylcholinesterase inhibitors are effective at treating and managing testicular dysfunction [33,54].

The energy requirement for spermatogenesis and sperm motility has been attributed to the significance of ATP and adenosine in male fertility [56,57]. They also increase sperm's capacity for capacitation and fertilization [58]. According to Fig. 6a, which shows

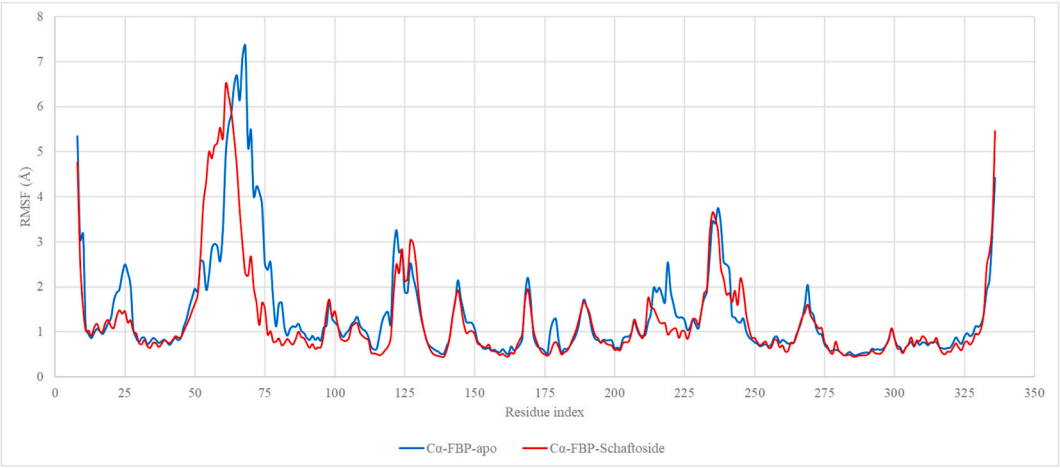

Fig. 10. Root Mean Squared Fluctuation RMSF from the MDS for 200ns for FBP-apoprotein aligned with the RMSF for the FBP in FBP-Schaftoside complex system.

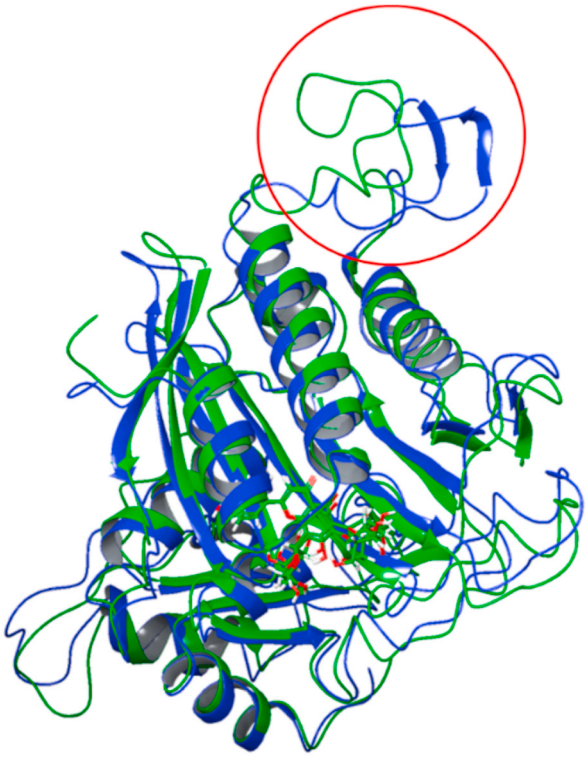

Fig. 11. Alignment of trajectory frame before (green) and after (blue) the dynamic loop conformation change. (For interpretation of the references to colour in this figure legend, the reader is referred to the Web version of this article.)

elevated ATPase activity in testis that have not been treated, oxidative injury results in a reduction in ATP levels. Similar to this, adenosine levels are depleted as shown by the reduced ENTPDase activity, implying a decreased energy supply for the typical physiological processes required for spermatogenesis as well as altered purinergic activities. The increased ATP and adenosine levels shown by the reversed activities in tissues treated with B. vulgaris leaf extracts suggest the availability of energy for the testes' regular physiological functions. This study is consistent with the reports of [40].

Male fertility has been reported to be significantly influenced by the glycolytic pathway in intermediary metabolism that produces ATP [59,60]. Its disruption has been linked to testicular toxicity [60]. In this study, increased G6Pase and F-1,6-BPase activities in untreated testicular tissues show a switch from glycolytic to gluconeogenic activity in the testes, favoring oxidative injury. Since both

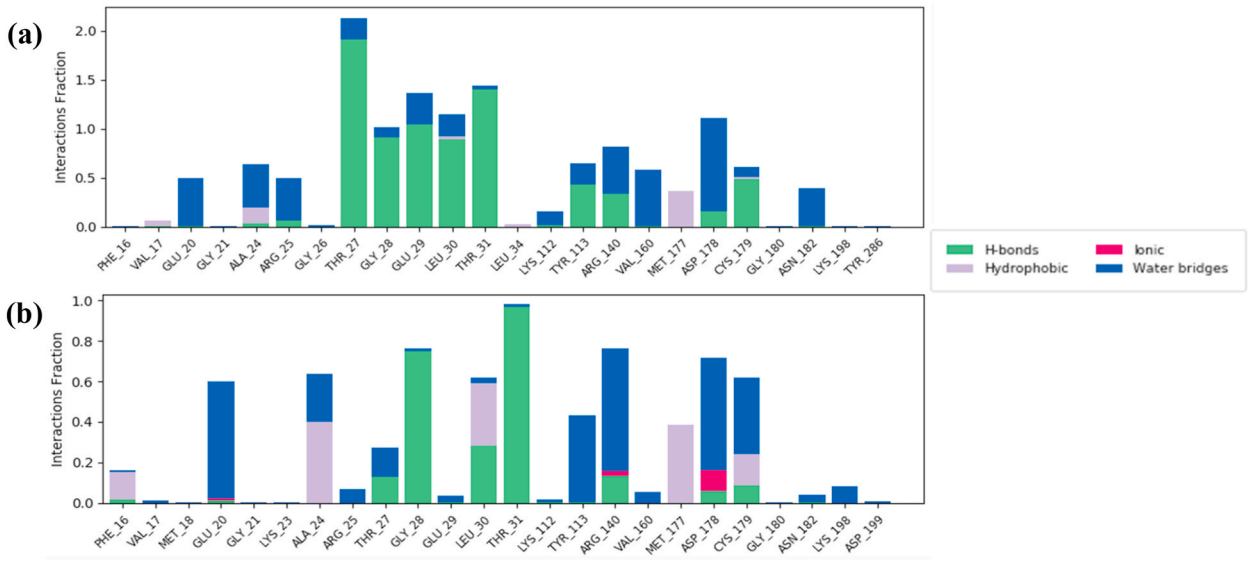

Fig. 12. FBP interactions with the (a) Schaftoside and (b) Quercetin throughout the simulation.

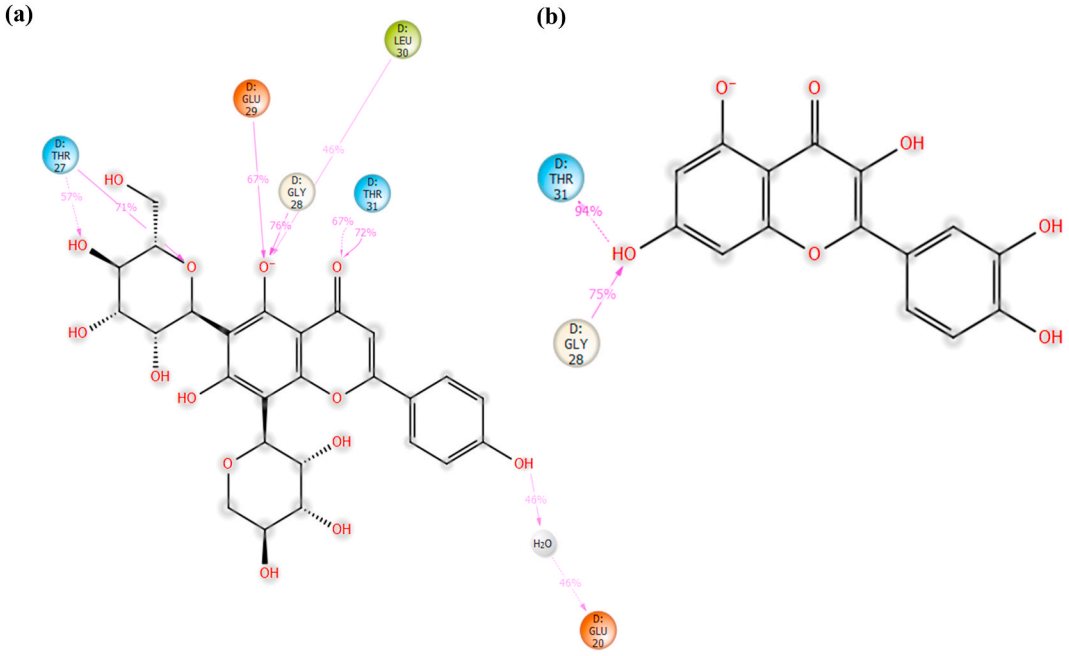

Fig. 13. Ligand-protein contacts for (a) FBP-Schaftoside and (b) FBP-Quercetin hydrogen bond interaction for at least 45% of the simulation time.

Table 5
Post-MDS binding free energy ΔGbind.

S/N	Compounds	ΔGbind (Kcal/mol)
1	Schaftoside	−53.13 ± 34.33 *
2	Quercetin	−31.09 ± 21.73

*$p < 0.01$ in comparison with quercetin (student t-test).

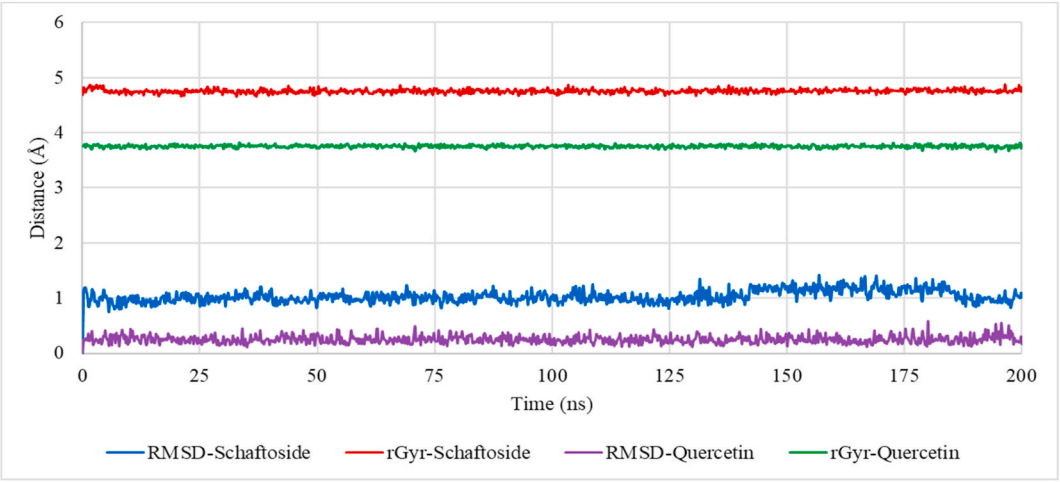

Fig. 14. Schaftoside and Quercetin properties throughout the simulation (root mean squared deviation, RMSD and radius of gyration, rGyr).

enzymes catalyze the reaction of G6P and F-1,6 B P to glucose and F-6-P, respectively, it can be said that gluconeogenesis results in an increased production of glucose.

This is consistent with earlier studies showing that these enzymes are more active in hyperglycemia-induced testicular toxicity [60], suggesting a disruption in the liberation of ATP during glycolysis and thus showing reduced levels of ATP during the induction of oxidative impairment. The continuous activity of these enzymes will cause a buildup of glucose in the testicles, which is harmful because glucose in its enediol form can act as a starting point for the production of free radicals [61]. As a result, the reversible activities of F-1,6-BPase and G-6-Pase after treatment with B. vulgaris extracts suggest a potential defense against disrupted carbohydrate metabolism caused by oxidative stress in testicular tissues.

Male fertility has been reported to be significantly influenced by the glycolytic pathway in intermediary metabolism that produces ATP [59,60]. Iron-induced oxidative stress may cause testicular damage and thus testicular dysfunction [62,63]. Glucose metabolism is an important event in spermatogenesis [64]. Because gluconeogenesis in the liver is a primary cause of glucose overproduction in diabetes, inhibiting FBP, a key enzyme in the gluconeogenesis pathway, appears to be a viable strategy to reduce hyperglycaemia that causes oxidative stress. FBP is allosterically regulated, and researchers have attempted to emulate the allosteric inhibitory effects of its natural inhibitor, AMP.

The top two molecules from our docking studies were schaftoside and quercetin (−53.82 and −51.18 kcal/mol, respectively). These compounds were investigated for MDS since binding free energy is a better ranking parameter for overall ligand binding quality than docking score. The simulations were performed for 200 ns and the interaction of schaftoside appears to have a more stable interaction with the target than quercetin.

In the FBP-Schaftoside complex simulation, the system appears to equilibrate from 10 ns, and schaftoside was stable in the binding pocket onward. The higher RMSD observed for FBP at about 130 ns (Fig. 9a) suggests a structural or conformational change within it in the FBP-Schaftoside complex system. Since Schaftoside was bound stably at the allosteric site, it may have triggered a conformational change at a different site on the FBP. The RMSF chart showed that a loop region (from about residue 50 to 75) was distorted, which could explain the significant increase in protein RMSD. Indeed, studies have revealed that FBP residues 50–72 form a dynamic loop that is required for its catalytic activity [65,66]. When coupled to the allosteric site, AMP, a natural physiological allosteric inhibitor of FBP [67], can promote the disengagement of the dynamic loop, resulting in inhibition [68]. These findings strongly suggest that Schaftoside is a potent FBP allosteric inhibitor. For the entire simulation, the average RMSD of schaftoside with respect to FBP was 3.07 $\pm$ 0.39 Å and quercetins was 5.70 $\pm$ 0.76 Å (P-value $<$0.0001), which suggests that schaftoside has a better proximity to the allosteric site.

Hydrogen bonding interactions between FBP and schaftoside were shown to be dominant at THR_27, GLY_28, GLU_29, LEU_30 and THR_31. It is worth noting that the authors of the FBP X-ray structure (7EZF) utilized zero-indexing for the protein's primary structure, so the five residues stated in the previous sentence are actually THR_28, GLY_29, GLU_30, LEU_31 and THR_32. These residues have been identified as the binding residues for FBP's physiological allosteric inhibitor, AMP [68], which are located some 47 Å away from the dynamic loop and 30 Å from the active site. The interaction fraction of quercetin with FBP was considerably less than that of Schaftoside. Only one hydroxyl group on quercetin maintained a hydrogen bond interaction with two residues, GLY_28 and THR_31, implying a weaker interaction when compared to schaftoside. The ligands' RMSD and radius of gyration suggest that the ligands' structures with respect to their heavy atoms were maintained throughout the simulation, and these indicate that both schaftoside and quercetin are in themselves stable under the simulation conditions.

5. Conclusion

Finally, the data obtained in this study imply that B. vulgaris leave extract may be employed in a variety of ways to treat oxidative testicular injury. The ability of B. vulgaris extract to reduce oxidative stress and pro-inflammatory responses, halt cholinergic dysfunction, control nucleotide hydrolysis, and modulate metabolic pathways all points to the therapeutic and protective potential of B. vulgaris extract on oxidative testicular injury. Additionally, the molecular docking and MDS analysis of the present study indicate that schaftoside may be an effective allosteric inhibitor of fructose 1,6-bisphosphatase based on the interacting residues and the subsequent effect on the dynamic loop conformation. However, further studies on the optimization of schaftoside, a potential lead compound in this study, may be required.

Author contribution statement

Oluwafemi Adeleke Ojo: Analyzed and interpreted the data; Conceived and designed the experiments; Contributed reagents, materials, analysis tools or data; Wrote the paper.

Joy Folashade Ayeni: Conceived and designed the experiments; Performed the experiments.

Adebola Busola Ojo: Conceived and designed the experiments; Analyzed and interpreted the data; Wrote the paper.

Matthew Iyobhebhe: Performed the experiments; Analyzed and interpreted the data; Wrote the paper.

Tobiloba Christiana Elebiyo, Damilare Emmanuel Rotimi: Performed the experiments; Contributed reagents, materials, analysis tools or data; Wrote the paper.

Anthonia Oluyemi Agboola, Olalekan Ogunro, Adeshina Isaiah Odugbemi, Samuel Ayodele Egieyeh, Olarewaju Michael Oluba: Performed the experiments; Analyzed and interpreted the data; Contributed reagents, materials, analysis tools or data; Wrote the paper.

Data availability statement

Data will be made available on request.

Funding

No funding was received.

Declaration of competing interest

The authors declare that they have no known competing financial interests or personal relationships that could have appeared to influence the work reported in this paper

Acknowledgment

Authors would like to acknowledge the National Integrated Cyberinfrastructure system (NICIS), Center for High Performance Computing (CHPC), Department of Science and Technology (DST), Republic of South Africa for the license to the Lengau Cluster and modules of the Schrödinger suite.

References

[1] M. Van Hemelrijck, A. Kessler, S. Sollie, B. Challacombe, K. Briggs, The global prevalence of erectile dysfunction: a review, BJU Int. 124 (2019) 587–599.
[2] S. Kerie, Y. Workineh, A.S. Kasa, E. Ayalew, M. Menberu, Erectile dysfunction among testicular cancer survivors: a systematic review and meta-analysis, Heliyon 7 (2021), e07479, https://doi.org/10.1016/j.heliyon.2021.e07479.
[3] M. Voznesensky, K. Annam, K.J. Kreder, Understanding and managing erectile dysfunction in patients treated for cancer, J. Oncol. Pract. 12 (2016) 297–304.
[4] F.A. Yafi, L. Jenkins, M. Albersen, G. Corona, A.M. Isidori, S. Goldfarb, M. Maggi, C.J. Nelson, S. Parish, A. Salonia, Erectile dysfunction, Nat. Rev. Dis. Prim. 2 (2016) 1–20.
[5] I.A. Ibrahim, A.A. Shalaby, R.T. Abd Elaziz, H.I. Bahr, Chlorella vulgaris or Spirulina platensis mitigate lead acetate-induced testicular oxidative stress and apoptosis with regard to androgen receptor expression in rats, Environ. Sci. Pollut. Control Ser. 28 (2021) 39126–39138.
[6] O.L. Erukainure, V.F. Salau, A.B. Oyenihi, N. Mshicileli, C.I. Chukwuma, M.S. Islam, Strawberry fruit (Fragaria x ananassa Romina) juice attenuates oxidative imbalance with concomitant modulation of metabolic indices linked to male infertility in testicular oxidative injury, Andrologia 53 (2021), e14175.
[7] K.A. Olofinsan, V.F. Salau, O.L. Erukainure, M.S. Islam, Ocimum tenuiflorum mitigates iron-induced testicular toxicity via modulation of redox imbalance, cholinergic and purinergic dysfunctions, and glucose metabolizing enzymes activities, Andrologia 53 (2021), e14179.
[8] N. Asadi, M. Bahmani, A. Kheradmand, M. Rafieian-Kopaei, The Impact of oxidative stress on testicular function and the role of antioxidants in improving it: a review, J. Clin. Diagn. Res. 11 (2017) IE01–IE05, https://doi.org/10.7860/JCDR/2017/23927.9886.
[9] M.G. Showell, J. Brown, A. Yazdani, M.T. Stankiewicz, R.J. Hart, Antioxidants for male subfertility, Cochrane Database Syst. Rev. (2011), https://doi.org/10.1002/14651858.CD007411.pub2.
[10] T.M. Said, A. Agarwal, R.K. Sharma, A.J. Thomas Jr., S.C. Sikka, Impact of sperm morphology on DNA damage caused by oxidative stress induced by beta-nicotinamide adenine dinucleotide phosphate, Fertil. Steril. 83 (2005) 95–103, https://doi.org/10.1016/j.fertnstert.2004.06.056.
[11] S. Venkatesh, J. Thilagavathi, K. Kumar, D. Deka, P. Talwar, R. Dada, Cytogenetic, Y chromosome microdeletion, sperm chromatin and oxidative stress analysis in male partners of couples experiencing recurrent spontaneous abortions, Arch. Gynecol. Obstet. 284 (2011) 1577–1584, https://doi.org/10.1007/s00404-011-1990-y.

[12] S. Akomolafe, G. Oboh, T. Olasehinde, S. Oyeleye, O. Ogunsuyi, Modulatory effects of Aqueous extract from Tetracarpidium conophorum leaves on key enzymes linked to erectile dysfunction and oxidative stress-induced lipid peroxidation in penile and testicular tissues, J. Appl. Pharmaceut. Sci. (2017) 51–56, https://doi.org/10.7324/japs.2017.70107.

[13] E.A. Abd El-Ghffar, N.M. Hegazi, H.H. Saad, M.M. Soliman, M.A. El-Raey, S.M. Shehata, A. Barakat, A. Yasri, M. Sobeh, HPLC-ESI- MS/MS analysis of beet (Beta vulgaris) leaves and its beneficial properties in type 1 diabetic rats, Biomed. Pharmacother. 120 (2019), 109541, https://doi.org/10.1016/j.biopha.2019.109541.

[14] N.K. Jain, A.K. Singhai, Protective role of Beta vulgaris L. leaves extract and fractions on ethanol-mediated hepatic toxicity, Acta Pol. Pharm. 69 (2012) 945–950.

[15] R.M. Martinez, D.T. Longhi-Balbinot, A.C. Zarpelon, L. Staurengo-Ferrari, M.M. Baracat, S.R. Georgetti, R.C. Sassonia, W.A. Verri, R. Casagrande, Anti-inflammatory activity of betalain-rich dye of Beta vulgaris: effect on edema, leukocyte recruitment, superoxide anion and cytokine production, Arch Pharm. Res. (Seoul) 38 (2015) 494–504, https://doi.org/10.1007/s12272-014-0473-7.

[16] S.H. Mohammed, M.M. Abdel-Aziz, S.M. Abu-Baker, M.A. Saad, A.M. Mohamed, A.M. Ghareeb, Antibacterial and potential antidiabetic activities of flavone C-glycosides isolated from beta vulgaris subspecies cicla L. Var. Flavescens (Amaranthaceae) cultivated in Egypt, Curr. Pharmaceut. Biotechnol. 20 (2019) 595–604, https://doi.org/10.2174/1389201020666190613161212.

[17] H. Szaefer, V. Krajka-Kuźniak, E. Ignatowicz, T. Adamska, W. Baer-Dubowska, Evaluation of the effect of beetroot juice on DMBA-induced damage in liver and mammary gland of female sprague–dawley rats, Phytother Res. 28 (2014) 55–61, https://doi.org/10.1002/ptr.4951.

[18] T. Albrahim, Silver nanoparticles-induced nephrotoxicity in rats: the protective role of red beetroot (Beta vulgaris) juice, Environ. Sci. Pollut. Control Ser. 27 (2020) 38871–38880.

[19] M.N. Alam, N.J. Bristi, M. Rafiquzzaman, Review on in vivo and in vitro methods evaluation of antioxidant activity, Saudi Pharmaceut. J. 21 (2013) 143–152.

[20] Z. Mzoughi, H. Chahdoura, Y. Chakroun, M. Cámara, V. Fernández-Ruiz, P. Morales, H. Mosbah, G. Flamini, M. Snoussi, H. Majdoub, Wild edible Swiss chard leaves (Beta vulgaris L. var. cicla): nutritional, phytochemical composition and biological activities, Food Res. Int. 119 (2019) 612–621.

[21] M.M. Rahman, M.B. Islam, M. Biswas, A.H. Khurshid Alam, In vitro antioxidant and free radical scavenging activity of different parts of Tabebuia pallida growing in Bangladesh, BMC Res. Notes 8 (2015) 621, https://doi.org/10.1186/s13104-015-1618-6.

[22] O.L. Erukainure, C.I. Chukwuma, M.G. Matsabisa, V.F. Salau, N.A. Koorbanally, M.S. Islam, Buddleja saligna Willd (Loganiaceae) inhibits angiotensin-converting enzyme activity in oxidative cardiopathy with concomitant modulation of nucleotide hydrolyzing enzymatic activities and dysregulated lipid metabolic pathways, J. Ethnopharmacol. 248 (2020), 112358.

[23] V.F. Salau, O.L. Erukainure, M. Islam, Caffeic acid protects against iron-induced cardiotoxicity by suppressing angiotensin-converting enzyme activity and modulating lipid spectrum, gluconeogenesis and nucleotide hydrolyzing enzyme activities, Biol. Trace Elem. Res. 199 (2021) 1052–1061.

[24] B.O. Ajiboye, B.E. Oyinloye, P.E. Agboinghale, O.A. Ojo, Cnidoscolus aconitifolius (Mill.) IM Johnst leaf extract prevents oxidative hepatic injury and improves muscle glucose uptake ex vivo, J. Food Biochem. 43 (2019), e13065.

[25] O.L. Erukainure, R. Mopuri, O.A. Oyebode, N.A. Koorbanally, M.S. Islam, Dacryodes edulis enhances antioxidant activities, suppresses DNA fragmentation in oxidative pancreatic and hepatic injuries; and inhibits carbohydrate digestive enzymes linked to type 2 diabetes, Biomed. Pharmacother. 96 (2017) 37–47.

[26] F.O. Balogun, A.O.T. Ashafa, Aqueous root extracts of Dicoma anomala (Sond.) extenuates postprandial hyperglycaemia in vitro and its modulation on the activities of carbohydrate-metabolizing enzymes in streptozotocin-induced diabetic Wistar rats, South Afr. J. Bot. 112 (2017) 102–111, https://doi.org/10.1016/j.sajb.2017.05.014.

[27] J.R. Greenwood, D. Calkins, A.P. Sullivan, J.C. Shelley, Towards the comprehensive, rapid, and accurate prediction of the favorable tautomeric states of drug-like molecules in aqueous solution, J. Comput. Aided Mol. Des. 24 (6–7) (2010) 591–604, https://doi.org/10.1007/s10822-010-9349-1.

[28] X. Wang, R. Zhao, W. Ji, J. Zhou, Q. Liu, L. Zhao, Z. Shen, S. Liu, B. Xu, Discovery of novel indole derivatives as fructose-1,6-bisphosphatase inhibitors and X-ray cocrystal structures analysis, ACS Med. Chem. Lett. 13 (1) (2022) 118–127, https://doi.org/10.1021/acsmedchemlett.1c00613.

[29] G.M. Sastry, M. Adzhigirey, T. Day, R. Annabhimoju, W. Sherman, Protein and ligand preparation: parameters, protocols, and influence on virtual screening enrichments, J. Comput. Aided Mol. Des. 227 (3) (2013) 221–234, https://doi.org/10.1007/s10822-013-9644-8.

[30] P.D. Lyne, M.L. Lamb, J.C. Saeh, Accurate prediction of the relative potencies of members of a series of kinase inhibitors using molecular docking and MM-GBSA scoring, J. Med. Chem. 49 (16) (2006) 4805–4808, https://doi.org/10.1021/jm060522a.

[31] O.A. Ojo, R.T. Aruleba, T.A. Adekiya, N.R. Sibuyi, A.B. Ojo, B.O. Ajiboye, B.E. Oyinloye, H.A. Adeola, A.O. Fadaka, Deciphering the interaction of Puerarin with cancer macromolecules: an in silico investigation, J. Biomol. Struct. Dyn. 40 (2) (2022) 848–859.

[32] A.O. Fadaka, O.A. Taiwo, O.A. Dosumu, O.P. Owolabi, A.B. Ojo, N.R.S. Sibuyi, S. Ullah, A.M. Madiehe, A. Klein, M. Meyer, O.A. Ojo, Computational prediction of potential drug-like compounds from cannabis sativa plant extracts targeted towards alzheimer therapy, J. Mol. Lipids (2022), 119393, https://doi.org/10.1016/j.molliq.2022.119393.

[33] O.L. Erukainure, O. Atolani, P. Banerjee, R. Abel, O.J. Pooe, O.S. Adeyemi, R. Preissner, C.I. Chukwuma, N.A. Koorbanally, M.S. Islam, Oxidative testicular injury: effect of l-leucine on redox, cholinergic and purinergic dysfunctions, and dysregulated metabolic pathways, Amino Acids (2021), https://doi.org/10.1007/s00726-021-02954-4.

[34] O.L. Erukainure, O. Sanni, M.S. Islam, Clerodendrum volubile: phenolics and applications to health, in: R.R. Watson, V.R. Preedy, S. Zibadi (Eds.), Polyphenols: Mechanisms of Action in Human Health and Disease, Elsevier, Amsterdam, Netherlands, 2018, pp. 53–68, https://doi.org/10.1016/b978-0-12-813006-3.00006-4.

[35] V.F. Salau, O.L. Erukainure, C.U. Ibeji, T.A. Olasehinde, N.A. Koorbanally, M.S. Islam, Vanillin and vanillic acid modulate antioxidant defense system via amelioration of metabolic complications linked to Fe 2+-induced brain tissues damage, Metab. Brain Dis. 35 (5) (2020) 727–738, https://doi.org/10.1007/s1101 1-020-00545-y.

[36] O.A. Ojo, J. Amanze, A.P. Oni, S. Grant, M. Iyobhebhe, T.C. Elebiyo, D. Rotimi, N.T. Asogwa, B.E. Oyinloye, B.E. Ajiboye, A.B. Ojo, Antidiabetic activity of avocado seeds (Persea americana Mill.) in diabetic rats via activation of PI3K/AKT signaling pathway, Sci. Rep. 12 (2022) 2919, https://doi.org/10.1038/s41598-022-07015-8.

[37] K. Sulakhiya, V.K. Patel, R. Saxena, J. Dashore, A.K. Srivastava, M. Rathore, Effect of Beta vulgaris Linn leaves extract on anxiety-and depressive-like behavior and oxidative stress in mice after acute restraint stress, Pharm. Res. (N. Y.) 8 (2016) 11–12.

[38] S. Jain, V.K. Garg, P.K. Sharma, Anti-inflammatory activity of aqueous extract of Beta vulgaris L, J. Basic Clin. Pharm. 2 (2012) 83–89.

[39] O.A. Ojo, A. Oni, S. Grant, J. Amanze, A.B. Ojo, O.A. Taiwo, R.F. Maimako, I.O. Evbuomwan, M. Iyobhebhe, C.O. Nwonuma, O. Osemwegie, Antidiabetic activity of elephant grass (Cenchrus purpureus (Schumach.) Morrone) via activation of PI3K/AkT signaling pathway, oxidative stress inhibition, and apoptosis in Wistar rats, Front. Pharmacol. (2022) 651.

[40] O.L. Erukainure, M.G. Matsabisa, V.F. Salau, J.O. Erhabor, M.S. Islam, Cannabis sativa L. Mitigates oxidative stress and cholinergic dysfunction; and modulates carbohydrate metabolic perturbation in oxidative testicular injury, Comp. Clin. Pathol. (2021) 1–13.

[41] B.O. Ajiboye, B.E. Oyinloye, O.A. Ojo, O.E. Lawal, Y.A. Jokomba, B.A. Balogun, A.O. Adeoye, O.R. Ajuwon, Effect of flavonoid-rich extract from dalbergiella welwitschii leaf on redox, cholinergic, monoaminergic, and purinergic dysfunction in oxidative testicular injury: ex vivo and in silico studies, Bioinf. Biol. Insights 16 (2022) 1–17, https://doi.org/10.1177/11779322221115546.

[42] B. Salehi, M. Martorell, J.L. Arbiser, A. Sureda, N. Martins, P.K. Maurya, M. Sharifi-Rad, P. Kumar, J. Sharifi-Rad, Antioxidants: positive or negative actors? Biomolecules 8 (4) (2018) 124, https://doi.org/10.3390/biom8010004.

[43] S. Hajihosseini, M. Setorki, Z. Hooshmandi, The antioxidant activity of Beta vulgaris leaf extract in improving scopolamine-induced spatial memory disorders in rats, Avicenna J. Phytomed. 7 (5) (2017) 417–425.

[44] L. Mahajan, P.K. Verma, R. Raina, S. Sood, Potentiating effect of imidacloprid on arsenic-induced testicular toxicity in Wistar rats, BMC Pharmacol. Toxicol. 19 (1) (2018) 1–8.

[45] M.-J. Chen, S.-S.-F. Peng, M.-Y. Lu, Y.-L. Yang, S.-T. Jou, H.-H. Chang, S.-U. Chen, D.-T. Lin, K.-H. Lin, Effect of iron overload on impaired fertility in male patients with transfusion-dependent beta-thalassemia, Pediatr. Res. 83 (3) (2018) 655–661.

[46] J.J. Pignatello, E. Oliveros, A. MacKay, Advanced oxidation processes for organic contaminant destruction based on the Fenton reaction and related chemistry, Crit. Rev. Environ. Sci. Technol. 36 (1) (2006) 1–84.
[47] C. Thomas, M.M. Mackey, A.A. Diaz, D.P. Cox, Hydroxyl radical is produced via the Fenton reaction in submitochondrial particles under oxidative stress: implications for diseases associated with iron accumulation, Redox Rep. 14 (3) (2009) 102–108.
[48] T.K. Das, M.R. Wati, K. Fatima-Shad, Oxidative stress gated by Fenton and Haber Weiss reactions and its association with Alzheimer's disease, Arch. Neurosci. 2 (2) (2015), e20078.
[49] S. McCann, C. Mastronardi, A. Walczewska, S. Karanth, V. Rettori, W. Yu, The role of nitric oxide in reproduction, Braz. J. Med. Biol. Res. 32 (11) (1999) 1367–1379.
[50] N.P. Lee, C.Y. Cheng, Nitric oxide and cyclic nucleotides: their roles in junction dynamics and spermatogenesis, in: C.Y. Cheng (Ed.), Molecular Mechanisms in Spermatogenesis, Advances in Experimental Medicine and Biology, vol. 636, Springer, New York, NY, 2009, pp. 172–185.
[51] Q. Yu, T. Li, J. Li, L. Zhong, X. Mao, Nitric oxide synthase in male urological and andrologic functions, in: S. Soheil, S. Saravi (Eds.), Nitric Oxide Synthase-Simple Enzyme-Complex Roles, IntechOpen, 2017.
[52] A. Azenabor, A.O. Ekun, O. Akinloye, Impact of inflammation on male reproductive tract, J. Reproduction Infertil. 16 (3) (2015) 123–129.
[53] I. Mor, H. Soreq, Cholinergic toxicity and the male reproductive system, in: Reproductive and Developmental Toxicology, Elsevier, 2011, pp. 863–870.
[54] O.A. Ojo, A.B. Ojo, B.E. Oyinloye, B.O. Ajiboye, O.O. Anifowose, A. Akawa, O.E. Olaiya, O.R. Olasehinde, A.P. Kappo, Ocimum gratissimum Linn. Leaves reduce the key enzymes activities relevant to erectile dysfunction in isolated penile and testicular tissues of rats, BMC Compl. Alternative Med. 19 (1) (2019) 1–10.
[55] K.-E. Andersson, Mechanisms of penile erection and basis for pharmacological treatment of erectile dysfunction, Pharm. Rev. 63 (4) (2011) 811–859.
[56] Y. Fan, Yu J. YuG, J. Sun, WuY, X. Zhao, Y. Meng, Z. He, C. Wang, Research trends and hotspots analysis related to the effects of xenobiotics on glucose metabolism in male testes, Int. J. Environ. Res. Publ. Health 15 (8) (2018) 1590.
[57] L. Rato, AlvesMG, S. Socorro, A.I. Duarte, J.E. Cavaco, P.F. Oliveira, Metabolic regulation is important for spermatogenesis, Nat. Rev. Urol. 9 (6) (2012) 330–338.
[58] G.I. Gorodeski, Purinergic signalling in the reproductive system, Auton. Neurosci. 191 (2015) 82–101.
[59] M. Alves, A. Martins, L. Rato, P. Moreira, S. Socorro, P. Oliveira, Molecular mechanisms beyond glucose transport in diabetes-related male infertility, Biochim. Biophys. Acta, Mol. Basis Dis. 1832 (5) (2013) 626–635.
[60] O.L. Erukainure, R. Reddy, M.S. Islam, Raffia Palm (Raphia hookeri) wine extenuates redox imbalance and modulates activities of glycolytic and cholinergic enzymes in hyperglycemia induced testicular injury in type 2 diabetes Rats, J. Food Biochem. 43 (2019), e12764.
[61] A. Maritim, R. Sanders, J. Watkins III, Diabetes, oxidative stress, and antioxidants: a review, J. Biochem. Mol. Toxicol. 17 (1) (2003) 24–38.
[62] C.C. Maresch, D.C. Stute, M.G. Alves, P.F. Oliveira, D.M. de Kretser, T. Linn, Diabetes-induced hyperglycemia impairs male reproductive function: a systematic review, Hum. Reprod. Update 24 (1) (2018) 86–105, https://doi.org/10.1093/humupd/dmx033.
[63] X.-Y. Tang, Q. Zhang, D.-Z. Dai, H.-J. Ying, Q.-J. Wang, Y. Dai, Effects of strontium fructose 1,6-diphosphate on expression of apoptosis-related genes and oxidative stress in testes of diabetic rats: FDP-Sr improves diabetic testis injury, Int. J. Urol. 15 (3) (2008) 251–256, https://doi.org/10.1111/j.1442-2042.2007.01980.x.
[64] M. Al-Maghrebi, W.M. Renno, Altered expression profile of glycolytic enzymes during testicular ischemia reperfusion injury is associated with the p53/TIGAR pathway: effect of fructose 1,6-diphosphate, PeerJ 4 (2016), e2195, https://doi.org/10.7717/peerj.2195.
[65] J.-Y. Choe, H.J. Fromm, R.B. Honzatko, Crystal structures of fructose 1,6-bisphosphatase: mechanism of catalysis and allosteric inhibition revealed in product complexes, Biochemistry 39 (29) (2000) 8565–8574, https://doi.org/10.1021/bi000574g.
[66] Y. Gao, C.V. Iancu, S. Mukind, J.-Y. Choe, R.B. Honzatko, Mechanism of displacement of a catalytically essential loop from the active site of mammalian fructose-1,6-bisphosphatase, Biochemistry 52 (31) (2013) 5206–5216, https://doi.org/10.1021/bi400532n.
[67] G.A. Tejwani, Regulation of fructose-bisphosphatase activity, in: A. Meister (Ed.), Advances in Enzymology—And Related Areas of Molecular Biology, John Wiley & Sons, Inc, 2006, pp. 121–194, https://doi.org/10.1002/9780470122990.ch3.
[68] Y. Xue, S. Huang, J.Y. Liang, Y. Zhang, W.N. Lipscomb, Crystal structure of fructose-1,6-bisphosphatase complexed with fructose 2,6-bisphosphate, AMP, and Zn2+ at 2.0-A resolution: aspects of synergism between inhibitors, Proc. Natl. Acad. Sci. USA 91 (26) (1994) 12482–12486, https://doi.org/10.1073/pnas.91.26.12482.